Magnetic structure of the kagome mixed compound $(Co_{0.5}Ni_{0.5})_3V_2O_8$

2008 J. Phys.: Condens. Matter 20 235228

(http://iopscience.iop.org/0953-8984/20/23/235228)

J. Phys.: Condens. Matter **20** (2008) 235228 (6pp) doi:10.1088/0953-8984/20/23/235228

Magnetic structure of the kagome mixed compound $(Co_{0.5}Ni_{0.5})_3V_2O_8$

N Qureshi[1,2], H Fuess[1], H Ehrenberg[3], B Ouladdiaf[2], J Rodríguez-Carvajal[2], T C Hansen[2], Th Wolf[4], C Meingast[4], Q Zhang[4], W Knafo[4,5] and H v Löhneysen[4,5]

[1] Institute for Materials Science, University of Technology, D-64287 Darmstadt, Germany
[2] Institut Max von Laue-Paul Langevin, 38042 Grenoble Cedex 9, France
[3] Institute for Complex Materials, IFW Dresden, D-01069 Dresden, Germany
[4] Research Center Karlsruhe, Institute of Solid State Physics, D-76021 Karlsruhe, Germany
[5] Physics Institute, Karlsruhe University, D-76128 Karlsruhe, Germany

E-mail: navidq@st.tu-darmstadt.de

Received 6 February 2008, in final form 2 April 2008
Published 9 May 2008
Online at stacks.iop.org/JPhysCM/20/235228

Abstract

We report the magnetic structure of $(Co_{0.5}Ni_{0.5})_3V_2O_8$ (CNVO) deduced by single crystal neutron diffraction. This compound exhibits features which differ from that of its parent compounds, which are absolutely collinear along the *a* axis for $Co_3V_2O_8$ (CVO) or exhibit magnetic moments predominantly in the *a*–*b* plane with small components along *c* in the case of $Ni_3V_2O_8$ (NVO). The averaged magnetic moments of the statistically distributed Ni^{2+} and Co^{2+} ions in CNVO are oriented in the *a*–*c* plane and form loops of quasiferromagnetically coupled spins. These loops are connected along the *a* axis and separated along the *c* axis by cross-tie spins forming a quasiferromagnetic wave with the upper part of the respective neighbouring loops. The magnetic moments are sinusoidally modulated by the propagation vector $\mathbf{k} = (0.49, 0, 0)$ with an average amplitude of 1.59(1) μ_B for a magnetic ion on a cross-tie site and 1.60(1) μ_B for the spine site. In addition to neutron diffraction, specific heat and magnetization data, which confirm that the only magnetic phase transition above 1.8 K is the onset of antiferromagnetic order at $T_N = 7.4(1)$ K, are presented.

(Some figures in this article are in colour only in the electronic version)

1. Introduction

$(Co_{0.5}Ni_{0.5})_3V_2O_8$ (CNVO) represents a mixed compound of the well investigated transition metal (M) orthooxovanadates $Ni_3V_2O_8$ (NVO) and $Co_3V_2O_8$ (CVO) labelled as kagome staircase structures. These structures are characterized by edge-sharing MO_6 octahedra isolated by nonmagnetic VO_4 tetrahedra. The crystallographic structure (orthorhombic space group *Cmca* [1, 2]) is interesting with respect to the magnetic properties as the magnetic ions form buckled planes of corner-sharing isosceles triangles representing an anisotropic variation of the ideal kagome net. Within these buckled planes, the kagome staircases, cross-tie ions on crystallographic 4a sites, link the linear chains of spine ions on 8e sites (figure 1). Due to the reduced symmetry of the kagome staircase geometry with respect to the ideal plane net the degree of frustration is lowered leading to interesting magnetic phase diagrams and long-range ordered magnetic structures. Several magnetization and heat capacity studies have been published concerning the sequence of magnetic phase transitions in NVO [3–7] and CVO [3, 4, 7–11], from which [5, 6, 9–11] additionally contain magnetic structure models arising from neutron diffraction data. The magnetic structures of CVO have been found to be collinear along the *a* axis, while the magnetic moments predominantly lie in the *a*–*b* plane for NVO. Further studies on the magnetic properties of CVO by implanted muons [12] and inelastic neutron scattering [13] have been reported, while considerable work has been done on the multiferroic properties of NVO [14–17]. Concerning the mixed system $(Co_xNi_{1-x})_3V_2O_8$ a magnetic composition–temperature phase diagram derived by neutron powder diffraction has been presented in [18], which exhibits four magnetic phase transitions as a function of the composition parameter *x*. A preliminary phase diagram derived by single crystal heat

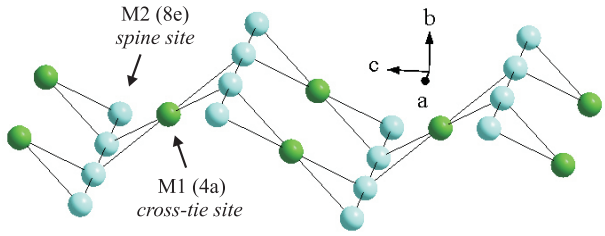

Figure 1. Illustration of a kagome staircase. Cross-tie ions on crystallographic 4a sites and spine ions on 8e sites are depicted in green (dark grey) and blue (light grey), respectively.

Table 1. Structural parameters of the investigated $(Co_{0.5}Ni_{0.5})_3V_2O_8$ single crystal sample.

Atom	x	y	z	B (Å^2)	Occupancy
Co1	0	0	0	0.11(5)	0.612(9)
Co2	0.25	0.1304(2)	0.25	0.12(5)	0.492(9)
Ni1	0	0	0	0.11(5)	0.388(9)
Ni2	0.25	0.1304(2)	0.25	0.12(5)	0.508(9)
V	0	0.3762	0.1196	0.24	1
O1	0	0.2489(3)	0.2306(5)	0.25(5)	1
O2	0	0.0012(3)	0.2451(5)	0.25(5)	1
O3	0.2673(3)	0.1193(2)	0.9988(5)	0.29(5)	1

Extinction parameters
Domain radius (nm): 1.4(1) Mosaicity spread (rad): 0.037(3)

capacity experiments has been shown in [19]. Magnetization and neutron diffraction experiments on a $(Co_{0.52}Ni_{0.48})_3V_2O_8$ powder sample [20] revealed only one temperature dependent magnetic phase transition into an antiferromagnetic ground state in contrast to the richness of magnetic phase transitions of its parent compounds. The magnetic structure is modulated by a composition dependent propagation vector $\mathbf{k} = (\delta, 0, 0)$ with δ being 0.491(4) for $(Co_{0.52}Ni_{0.48})_3V_2O_8$ where a similarity to the NVO type magnetic structure was assumed. The single crystal data presented here produce a more detailed picture of an interesting non-collinear magnetic structure.

2. Experimental details

A $(Co_{0.5}Ni_{0.5})_3V_2O_8$ single crystal was grown from self-flux in a ZrO_2/Y crucible by the slow cooling method. The structural investigation was performed at the four-circle diffractometer D10 (ILL, Grenoble). As no magnetic contribution from a zero wavevector is present on the nuclear reflections, both the nuclear and the magnetic structure were investigated at $T = 1.5$ K using a wavelength of 2.359 Å from a pyrolytic graphite monochromator. An additional data set of the nuclear reflections was collected with $\lambda = 1.255$ Å supplied by the (200) reflection of a Cu monochromator in order to be able to apply extinction and absorption corrections. By using a four-circle cryostat a large part of the reciprocal space could be investigated, offering the possibility of measuring a large number of reflections. Besides the structural investigations various scans in reciprocal space directions and in temperature were carried out in order to extract information about the a^*, b^* and c^* components of the propagation vector and the

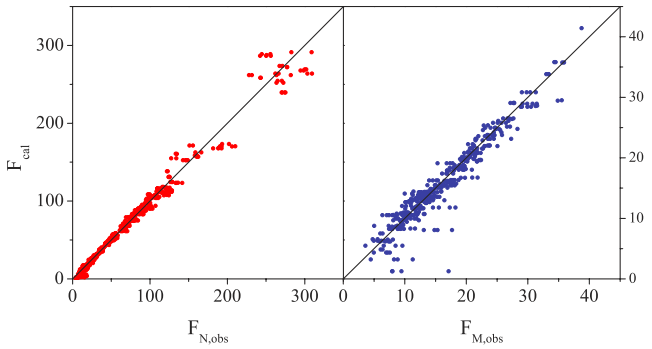

Figure 2. Illustration of the fit results. The left and right panels show the nuclear and magnetic data, respectively.

magnetic phase transition temperature. Magnetization curves were recorded on a SQUID magnetometer (Quantum Design) as a function of temperature, in 0.05 K steps, in a magnetic field of 50 Oe applied along the principal crystallographic axes. The specific heat was measured in zero field with a standard PPMS calorimeter from Quantum Design. The data close to the transition were obtained by using a procedure similar to that presented in [21], which allows for a high temperature resolution.

3. Results

3.1. Nuclear structure

The nuclear structure investigation confirmed the correct phase formation of the orthorhombic structure (space group *Cmca*). The cell constants were found to be $a = 5.981(2)$ Å, $b = 11.436(5)$ Å and $c = 8.261(6)$ Å, showing close agreement with the previously investigated powder sample with a similar composition [20]. The integrated intensities were corrected for absorption and extinction applying the transmission factor integral $\exp[-\mu(\tau_{in} + \tau_{out})]$ and the derivative integral $(\tau_{in} + \tau_{out})\exp[-\mu(\tau_{in} + \tau_{out})]$ according to the Becker and Coppens Lorentzian model [22] (τ_{in} and τ_{out} represent the path lengths of the beam inside the crystal before and after the diffraction process, μ is the linear absorption coefficient, which is 0.448 cm^{-1} for CNVO). The structural models were refined using programs of the Cambridge Crystallographic Subroutine Library [23] and confirmed by FullProf [24]. The nuclear structure refinement included the respective atomic positions and isotropic temperature factors of M and O plus the cation distribution of Co and Ni on both M sites and the extinction parameters. Because of its low coherent neutron scattering cross section, the atomic position and the temperature factor of V have been fixed in all refinements. The refined values ($R_1 = 6.4$) are listed in table 1. The goodness of the fit is illustrated by a F_{obs} versus F_{cal} plot in figure 2. The analysis of the cation occupancy yields a true Co:Ni ratio of 53:47 with the Co^{2+} ions having a higher affinity for the more symmetric 4a site as previously reported [11, 25].

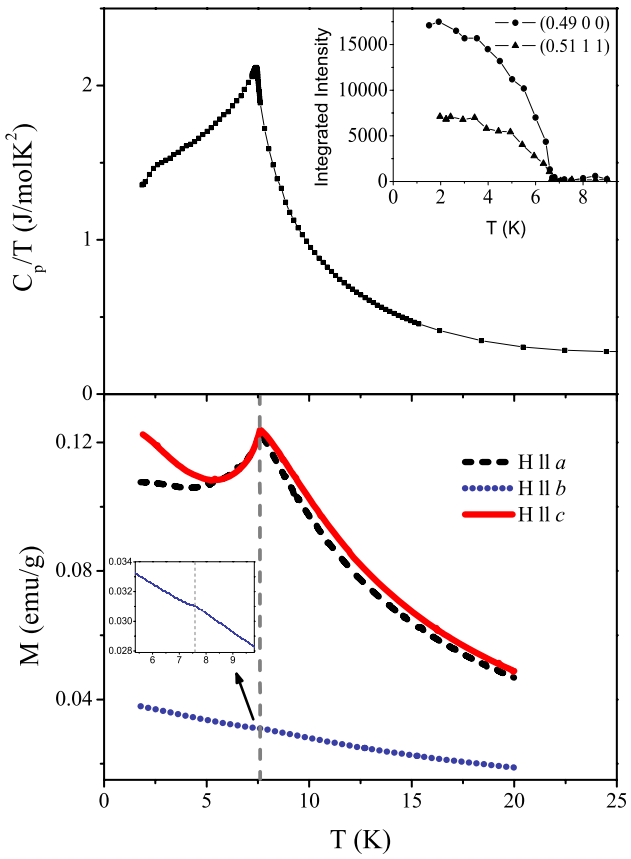

Figure 3. Upper panel: heat capacity curve as a function of temperature. The inset in the upper right corner displays the temperature dependence of the integrated intensities of two chosen magnetic reflections (data points in the upper panel and inset are connected by straight lines). Lower panel: magnetization curves of a $(Co_{0.5}Ni_{0.5})_3V_2O_8$ single crystal with $H = 50$ Oe applied parallel to the respective crystal axes. The inset indicated by an arrow shows a magnification to focus the transition point of the curve with $H \parallel b$.

3.2. Magnetic phase transition temperature

The investigation of the magnetic properties was first dedicated to examining the transition temperature. Therefore the $(000)^+$ and $(111)^-$ reflections were measured as a function of temperature to determine the transition temperature into the antiferromagnetic phase. It can be seen in the upper right inset of figure 3 that the magnetic reflections appear at approximately 6.8(2) K. Magnetization measurements with an applied magnetic field of 50 Oe parallel to the respective crystallographic axes exhibit anomalies of the magnetization curves at 7.6(1) K (lower panel of figure 3), which agrees well with the transition temperature of the powder sample [20] investigated on the same instrument. The specific heat is shown in the upper panel of figure 3 in a C_p/T versus T representation. The magnetic transition manifests itself as a sharp maximum in C_p/T at $T_N = 7.4(1)$ K, which we declare as the temperature of magnetic ordering as we consider the heat capacity to be the most precise of the data presented here for localizing the magnetic phase transition. The slightly different results in the magnetization and diffraction experiments are considered to be a result of the chosen criterion for determining the transition temperature. A magnetic signal extends in the specific heat data up to about 25 K, i.e. more than three times T_N. This could be the signature of magnetic fluctuations, whose nature is unknown. Similar short-range ordering effects up to about $3 \times T_N$ are also observed in $Cu_3V_2O_8$ [26] and may share a similar origin. Below T_N, C_p/T remains unusually high down to the lowest measured temperature of 1.8 K, probably because of magnetic fluctuations, a consequence of the frustration. Such a behaviour is sometimes observed in heavy-fermion systems, where strong fluctuations, due to Kondo and RKKY interactions, are present in the magnetically ordered phase [27]. At about 2.4 K we observe a 'bump' in the C_p/T data, the origin of which is not yet understood.

3.3. Propagation vector

In order to verify the propagation vector the $(000)^+$ reflection was scanned along the three principal directions of reciprocal space. The a^*, b^* and c^* components of the wavevector were deduced by determining the centres of pseudo-Voigt functions, which were fitted to the observed reflection profiles (figure 4). The resulting values confirm the propagation vector $\mathbf{k} = (0.49, 0, 0)$, where it has to be stressed that an incommensurability is present. This has been checked by verifying the position of the (400) reflection, which was found to be precisely centred at $h = 4.00$, and by further analysis of the powder data of [20].

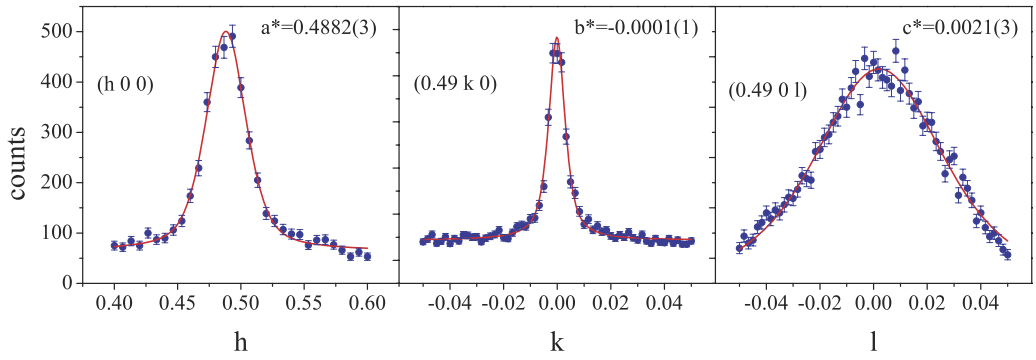

Figure 4. q-scans through the $(000)^+$ reflection along the a^*, b^* and c^* directions. The centres of the pseudo-Voigt fits are displayed in the upper right corners of the respective plots confirming the propagation vector $\mathbf{k} = (0.49, 0, 0)$.

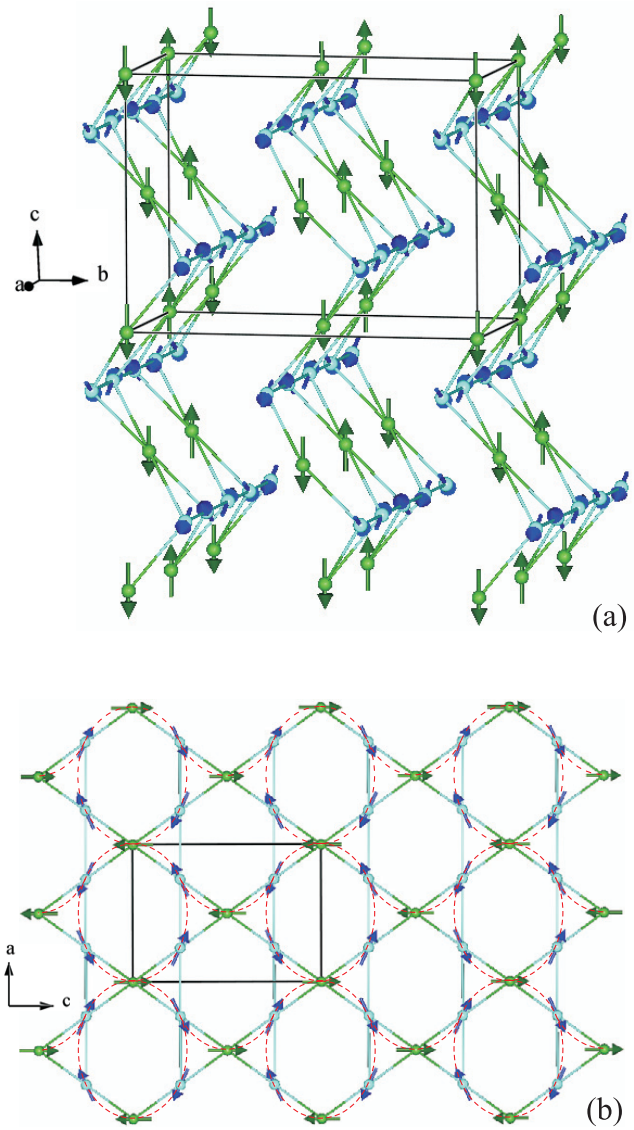

Figure 5. Antiferromagnetic structure model with $\mathbf{k} = (0.49, 0, 0)$: (a) shows the perspective view on three neighbouring staircases and (b) shows a single staircase viewed along the b axis revealing the quasiferromagnetic loops and waves (sketched with broken lines).

3.4. Magnetic structure

For the determination of the magnetic structure more than 400 independent magnetic reflections were measured. Magnetic structure models were obtained using representation analysis. The eight symmetry operators for the (000)+set of space group *Cmca* form the group G. Only four symmetry elements of group G leave the propagation vector $\mathbf{k} = (0.49, 0, 0)$ invariant, forming the little group $G_k = \{1, 2_x, b_{xy}, c_{xz}\}$. All the elements of G_k permute, which leads to four one-dimensional irreducible representations labelled Γ_1 to Γ_4 as denoted in [6]. The decompositions of the induced representations for the respective sites are $\Gamma(4a) = \Gamma^1 + \Gamma^2 + 2\Gamma^3 + 2\Gamma^4$ and $\Gamma(8e) = 3\Gamma^1 + 3\Gamma^2 + 3\Gamma^3 + 3\Gamma^4$. The observed integrated intensities are distinctly best described ($R_1 = 8.2$, see figure 2) by the magnetic mode $C_1(S_{1ay} - S_{1by}) + C_2(S_{1az} + S_{1bz}) + C_3(S_{2ax} + S_{2bx} - S_{2cx} - S_{2dx}) + C_4(S_{2ay} - S_{2by} - S_{2cy} + S_{2dy}) + C_5(S_{2az} + S_{2bz} + S_{2cz} + S_{2dz})$ corresponding to Γ^4, where $S_{i,n}$ represents a magnetic moment of atom n on site i (see table 2 for the definition of the respective atoms). The propagation of the magnetic mode is amplitude modulated by the wavevector $\mathbf{k} = (0.49, 0, 0)$. The parameters C_1 to C_5 have been set as variables in the refinement process, where an averaged magnetic form factor consisting of the weighted analytical approximations of the Ni^{2+} and Co^{2+} form factors has been used. In a first step, the refinement parameters C_1 and C_4 were found to be very small with relatively large standard deviations, indicating that the magnetic moments on both crystallographic sites probably do not exhibit a b component. For further refinement steps these variables were set to zero. However, an upper bound of $C_1 = 0.11(3)\ \mu_B$ and $C_4 = 0.15(6)\ \mu_B$ can be given for the 4a cross-tie and 8e spine moments, respectively [$C_2 = 1.59(2)\ \mu_B, C_3 = 1.44(2)\ \mu_B, C_5 = 0.65(1)\ \mu_B$]. Finally, the resulting amplitudes of the modulating waves have been refined to $1.59(1)\ \mu_B$ along the c axis for the cross-tie spins and $1.60(1)\ \mu_B$ within the a–c plane for the spine spins at 1.5 K. The angle θ between the spine magnetic moments and the c axis has been refined to 65.1(3)°. A phase shift between the modulating waves of the two magnetic sites results in a considerably worse fit and is therefore not justified. The magnetic structure is depicted in figure 5 and will be described in detail in section 4.

Table 2. Fractional coordinates of the M^{2+} ions related to the spin properties $S_{i,n}$ and the corresponding Fourier coefficients.

Site i	Atom n	x, y, z-coordinates	Fourier coefficients
1(4a)	a	$(0, 0, 0)$	$(0, v_1, w_1)$
	b	$(0, \frac{1}{2}, \frac{1}{2})$	$(0, -v_1, w_1)$
2(8e)	a	$(\frac{1}{4}, y, \frac{1}{4})$	(u_2, v_2, w_2)
	b	$(\frac{1}{4}, \bar{y} + \frac{1}{2}, \frac{3}{4})$	$(u_2, -v_2, w_2)$
	c	$(\frac{1}{4}, y + \frac{1}{2}, \frac{1}{4})$	$(-u_2, -v_2, w_2)$
	d	$(\frac{1}{4}, \bar{y}, \frac{3}{4})$	$(-u_2, v_2, w_2)$

4. Discussion

In the proposed magnetic structure of CNVO, which results from the same irreducible representation as the high temperature incommensurate phase of NVO and is modulated by the same type of propagation vector, the two sublattices of M^{2+} ions exhibit differently oriented magnetic moments in the a–c plane, where the cross-tie moments are collinear along the c axis but the spine moments span a 65.1(3)° angle with the c axis. As previously reported [5], the symmetry of the crystal structure admits a Dzyaloshinskii–Moriya interaction among the nearest neighbour spine spins, which justifies the observed canting between the aforementioned spins in CNVO. Figure 5 displays the magnetic structure after a global phase shift of $\frac{\pi}{4}$ has been applied in order to show a picture, in which the amplitude of all magnetic moments is sufficiently high so that their orientation is clearly visible. The 4a site is represented by green atoms (dark grey) and magnetic moments, while the 8e site is depicted in blue (light grey). Figure 5(b) shows a

single staircase viewed along the b axis, which emphasizes the characteristics of this magnetic structure. Given the orientation of the magnetic moments with respect to the crystal axes there exist in principle 2^3 possibilities to place the moments on the corners of the isosceles triangles of the kagome staircase structure. The magnetic structure presented here reveals only six of these possibilities. No triangle can be found in which all three moments point either towards or away from each other, as would be expected for a frustrated antiferromagnetic system. Due to the propagation vector $\mathbf{k} = (0.49, 0, 0)$ the direction of every magnetic moment is flipped after a translation of the lattice vector a. The resulting picture of the average magnetic structure shows loops, within which every pair of nearest neighbour spins couples as in a canted ferromagnet. We call this arrangement a quasiferromagnetic loop, because a ferromagnetic component exists for every pair of nearest neighbours but not for the whole loop. These loops are connected along the a axis with an alternating sense of rotation, while they are separated along the c axis by cross-tie moments not belonging to the loops but forming the same kind of canted ferromagnetic coupling with their nearest neighbour on the superior part of a loop on either side. This results in a sort of wave along the c axis, which also alternates its direction when translated by a. Similarly, we call this a quasiferromagnetic wave, because the ferromagnetic components of two neighbouring spins are not parallel for all pairs of neighbours. After a translation of $\pm 12.5a$, where the amplitudes of the magnetic moments run through the full value and zero, respectively, the loops are shifted by $(\frac{1}{2}, 0, \frac{1}{2})$, i.e. they trade places with the connecting segments. This switching has a period of $25a$. As the propagation vector possesses an a^* component the neighbouring kagome staircases do not differ concerning their spin arrangement like in the antiferromagnetic structure of CVO, where the staircases alternate between ferromagnetic and antiferromagnetic ones. It can be seen in figure 5(a) that the orientation of the spine spins within the chains along the a axis is exactly the same as in each of the two neighbouring chains of the next staircase. A mean-field approach to the first ordered state based on classical spins [28] was attempted in order to confirm the magnetic structure theoretically. The attempt failed because of the inability to adequately describe the vicinity of each magnetic moment, which varies locally as a consequence of the statistical occupation of the magnetic sites by Co and Ni.

As previously reported [20], only one magnetic phase transition could be observed down to 1.8 K, which our heat capacity measurements confirm. However, as an incommensurate magnetic structure is not likely to be a ground state, a commensurate lock-in is expected at very low temperatures.

5. Conclusions

The striking result of the work presented here is the considerable deviation of the CNVO magnetic structure from those of its parent compounds CVO and NVO, which exhibit a variety of magnetic structures with magnetic moments oriented along the a axis [9] or predominantly in the a–b plane with small components along c [6], respectively. Comparing the ground states of the parent compounds, which are a ferromagnet for CVO and a canted antiferromagnet for NVO, with the magnetic structure presented here, one can deduce a higher degree of competition between nearest neighbour interactions for CNVO. A simple global picture based on exchange interactions cannot be given, as a consequence of the chemical disorder. However, the Ising-like behaviour of Co^{2+} in combination with its higher affinity for the 4a site could explain the collinear alignment of the cross-tie spins. The results of this work should be followed by a theoretical approach as it shows once again that the competition between exchange interactions along various coupling pathways in this particular crystallographic system results in a variety of different interesting magnetic structures.

Acknowledgments

This research was supported by the Deutsche Forschungsgemeinschaft within the priority programme 1178. Support by the Helmholtz Association of German Research Centers under project VH-NG-016 is gratefully acknowledged.

References

[1] Fuess H, Bertaut E F, Pauthenet R and Durif A 1970 *Acta Crystallogr.* B **26** 2036
[2] Sauerbrei E E, Faggiani R and Calvo C 1973 *Acta Crystallogr.* B **29** 2304
[3] Rogado N, Lawes G, Huse D A, Ramirez A P and Cava R J 2002 *Solid State Commun.* **124** 229
[4] Balakrishnan G, Petrenko O A, Lees M R and Paul D M K 2004 *J. Phys.: Condens. Matter* **16** L347
[5] Lawes G *et al* 2004 *Phys. Rev. Lett.* **93** 247201
[6] Kenzelmann M *et al* 2006 *Phys. Rev.* B **74** 014429
[7] Wilson N R, Petrenko O A and Chapon L C 2007 *Phys. Rev.* B **75** 094432
[8] Szymczak R, Baran M, Diduszko R, Fink-Finowicki J, Gutowska M, Szewczyk A and Szymczak H 2006 *Phys. Rev.* B **73** 094425
[9] Chen Y *et al* 2006 *Phys. Rev.* B **74** 014430
[10] Wilson N R, Petrenko O A and Balakrishnan G 2007 *J. Phys.: Condens. Matter* **19** 145257
[11] Qureshi N, Fuess H, Ehrenberg H, Hansen T C and Schwabe D 2007 *Solid State Commun.* **142** 169
[12] Lancaster T, Blundell S J, Baker P J, Prabhakaran D, Hayes W and Pratt F L 2007 *Phys. Rev.* B **75** 064427
[13] Wilson N R, Petrenko O A, Balakrishnan G, Manuel P and Fak B 2007 *J. Magn. Magn. Mater.* **310** 1334
[14] Lawes G *et al* 2005 *Phys. Rev. Lett.* **95** 087205
[15] Harris A B, Yildirim T, Aharony A and Entin-Wohlman O 2006 *Phys. Rev.* B **73** 184433
[16] Rai R C, Cao J, Brown S, Musfeldt J L, Kasinathan D, Singh D J, Lawes G, Rogado N, Cava R J and Wei X 2007 *Phys. Rev.* B **76** 174414
[17] Chaudhury R P, Yen F, dela Cruz C R, Lorenz B, Wang Y Q, Sun Y Y and Chu C W 2007 *Phys. Rev.* B **75** 012407
[18] Qureshi N, Fuess H, Ehrenberg H, Hansen T C, Ritter C, Adelmann P, Meingast C, Wolf T, Zhang Q and Knafo W 2008 *J. Phys.: Condens. Matter* **20** 095219
[19] Zhang Q, Knafo W, Grube K, v Löhneysen H, Meingast C and Wolf T 2008 *Physica* B **403** 1404

[20] Qureshi N, Fuess H, Ehrenberg H, Hansen T C, Ritter C, Prokes K, Podlesnyak A and Schwabe D 2006 *Phys. Rev.* B **74** 212407
[21] Lashley J C *et al* 2003 *Cryogenics* **43** 369
[22] Becker P J and Coppens P 1974 *Acta Crystallogr.* A **30** 129
[23] Matthewman J C, Thompson P and Brown P J 1982 *J. Appl. Crystallogr.* **15** 167
[24] Rodríguez-Carvajal J 1993 *Physica* B **192** 55
[25] Wang P L, Werner P E and Nord A G 1992 *Z. Kristallogr.* **198** 271
[26] Rogado N, Haas M K, Lawes G, Huse D A, Ramirez A P and Cava R J 2003 *J. Phys.: Condens. Matter* **15** 907
[27] v Löhneysen H, Sieck M, Stockert O and Waffenschmidt M 1996 *Physica* B **223/224** 471
[28] Freiser M J 1961 *Phys. Rev.* **123** 2003